HHS Public Access

Author manuscript

J Surg Oncol. Author manuscript; available in PMC 2019 August 11.

Published in final edited form as:

J Surg Oncol. 2018 August ; 118(2): 344–355. doi:10.1002/jso.25149.

Intraoperative Fluorescence Imaging in Thoracic Surgery

Andrew D. Newton, MD[1], **Jarrod D. Predina, MD**[1], **Shuming Nie, PhD**[2], **Philip Low, PhD**[3], and **Sunil Singhal, MD**[1]

[1]Department of Surgery, University of Pennsylvania Perelman School of Medicine, Pennsylvania, PA

[2]Department of Bioengineering, University of Illinois at Urbana-Champaign, Urbana, IL

[3]Department of Chemistry, Purdue University, West Lafayette, IN

Abstract

Intraoperative fluorescence imaging (IFI) can improve real-time identification of cancer cells during an operation. Phase I clinical trials in thoracic surgery have demonstrated that IFI with second window indocyanine green (TumorGlow®) can identify sub-centimeter pulmonary nodules, anterior mediastinal masses, and mesothelioma, while use of a folate receptor-targeted near-infrared agent, OTL38, can improve the specificity for diagnosing tumors with folate receptor expression. Here we review the existing preclinical and clinical data on IFI in thoracic surgery.

Keywords

intraoperative fluorescence imaging; near-infrared fluorescence imaging; thoracic surgery; indocyanine green; OTL38

Introduction

The goal of a successful cancer operation is localization and accurate discrimination of malignant versus benign tissue to maximize removal of cancer while minimizing removal of non-cancerous tissue. Thoracic surgeons perform a wide variety of cancer operations, and each presents unique challenges in achieving this goal. Challenges in thoracic cancer operations include 1) identification of small primary, synchronous, or metachronous pulmonary nodules; 2) accurate selection of lymph nodes with metastatic disease during pulmonary resection or esophagectomy; 3) assessment of mediastinal mass margins and differentiation of tumor from surrounding critical structures such as the phrenic nerve; 4) recognition of residual disease following tumor debulking as in pleurectomy for mesothelioma.

Corresponding Author: Sunil Singhal, MD, Hospital of the University of Pennsylvania, Department of Surgery, 3400 Spruce Street, 6 White, Philadelphia, PA 19104, Sunil.Singhal@uphs.upenn.edu, Telephone: 215-662-4767.

Disclosures

There are no disclosures from the other authors.

Traditionally, thoracic surgeons have only had two intraoperative tools, visual inspection and manual palpation, to meet these challenges.(1) Intraoperative fluorescence imaging (IFI) is an emerging technology with the potential to dramatically improve oncologic operations. This technology requires (i) a fluorescent dye that will selectively accumulate in tumor tissues, and (ii) a specialized imaging system to detect and quantify the dye. Several features of IFI make it more attractive than other intraoperative adjuncts to a surgeon's hands, eyes, and clinical decision making during a tumor resection. First, it does not involve exposure to ionizing radiation. Second, the imaging is easy to interpret for surgeons unfamiliar with the technology. Third, IFI causes minimal interruption and integrates nicely into the normal flow of an operation. In this review, we summarize the existing preclinical and clinical data on IFI applications in thoracic surgery.

Preclinical Studies of Fluorescent Dyes for IFI

Three fluorescent dyes have been used in clinical trials to target patients with thoracic malignancies: indocyanine green (ICG) and two receptor-targeted agents, EC17 and OTL38. The feasibility and potential limitations of IFI with these dyes were first suggested by preclinical animal studies. ICG, a non-targeted near-infrared (NIR) contrast agent with excitation and emission wavelengths of approximately 805 nm and 830 nm and the only clinically approved NIR fluorophore, was the first dye studied. ICG has traditionally been used for vascular perfusion imaging; common applications include assessment of perfusion to tissue flaps and bowel anastomoses.(2, 3) When used to assess perfusion, a low dose of ICG (5–10 mg) is given as a bolus immediately prior to imaging. More recently, it has been demonstrated that NIR imaging with ICG can also detect hepatocellular carcinoma (HCC), colorectal and pancreatic cancer liver metastases, and sentinel lymph nodes in breast cancer and melanoma.(4–8) When used for liver tumors, a low to medium ICG dose ranging from 10 mg – 0.5 mg/kg is given 1–7 days before surgery. ICG, which is cleared hepatically, then accumulates within the tumors due to impaired biliary excretion. When used for sentinel lymph nodes, albumin-bound ICG (ICG:HSA) is given in peritumoral injections, and NIR imaging can highlight draining lymphatic channels and nodes.

Our group was the first to show that an alternative method of ICG delivery, the second window technique, can be used for NIR imaging of lung tumors.(9, 10) The second window technique is different from other methods of IFI with ICG in that a much higher dose (5 mg/kg) is given via slow infusion 24 hours prior to surgery. In order to differentiate it from IFI with low dose ICG as a perfusion agent, we coined the term TumorGlow® for IFI with ICG via the second window technique. The hypothesized mechanism of ICG accumulation in tumors using the second window technique is the enhanced permeability and retention (EPR) effect. The EPR effect is the concept that macromolecules cannot escape the tight junctions of normal capillaries but extravasate from the leaky capillaries of tumors.(11, 12) Due to properties such as size, shape, charge, and polarity, these macromolecules are then retained within the tumors.(13) Although ICG is a small molecule (0.775 kDa), it is 98% protein bound in circulation and therefore acts as a macromolecule.(14)

We initially demonstrated in mice that TumorGlow® is effective at identifying residual disease in a surgical wound not visible to the naked eye and that delineation of tumor

margins compared to normal tissue is very precise using this technology.(9) ICG will accumulate in murine models of several thoracic malignancies including lung cancer, esophageal cancer, thymoma, and mesothelioma.(9, 15, 16) In preclinical canine studies, we demonstrated that TumorGlow® can localize spontaneously occurring sarcomas and lung cancers.(17, 18) However, we also discovered one of the major limitations of TumorGlow®, which is poor discrimination between tumors and surrounding peritumoral inflammation. In one study of 8 canines with lung tumors, 5 dogs had no post-obstructive pneumonitis, and 3 dogs had large tumors with significant post-obstructive pneumonitis.(18) In the 5 dogs with no post-obstructive pneumonitis, tumors were highly fluorescent, and all fluorescence was within 5 mm of the tumor edge. Conversely, in the 3 dogs with post-obstructive pneumonitis, there was no difference in fluorescence between the tumor edge and 5 mm from the tumor, and there was significant fluorescence even at 10 mm from the tumor edge.

The limitations in ICG specificity including accumulation in areas of inflammation prompted us to seek a targeted molecular imaging agent that would specifically bind to and identify pulmonary adenocarcinoma. In collaboration with our co-author (PSL), we tested the first targeted IFI agent for thoracic surgery, EC17. EC17 is a folate analog conjugated to fluorescein isothiocyanate (FITC) with maximum excitation and emission wavelengths of 470 and 520 nm.(19) This ligand was chosen because the folate receptor-alpha (FRα) is highly expressed on certain malignancies of epithelial origin, including pulmonary adenocarcinomas.(20, 21) FRα is a cell surface glycoprotein with high affinity for 5-methyltetrahydrofolate, the primary plasma form of folate.(21) FRα has previously been targeted for folate conjugated chemotherapies and immunotherapies.(22–26) A fluorescein dye was chosen due to a long history of data demonstrating safety.(27–29)

We demonstrated in mice that EC17 can identify additional tumor deposits at the resection margins and is superior to traditional methods of hand palpation and sight at detecting residual disease in the wound bed.(30) The major limitations of EC17 in preclinical studies were poor depth of penetration and tissue auto-fluorescence due to fluorescence in the visible light spectrum.(19)

Thus, a third fluorescent dye, OTL38, was designed to improve on the limitations of EC17. OTL38 is a folate analog conjugated to the NIR dye S0456 with maximum excitation and emission of 776 and 796 nm.(31) In theory, it combines the major advantage of EC17, increased specificity, with the major advantages of NIR drugs such as ICG, increased depth of penetration and decreased auto-fluorescence. Increased depth of penetration into solid organs and decreased auto-fluorescence are seen in the NIR spectrum (700–900 nm) due to decreased light scatter and blood absorption.(32, 33) This improves discrimination between tumor tissues which are accumulating dye and normal tissues which are not accumulating dye to increase the signal-to-background ratio (SBR).

We directly compared OTL38 and EC17 in several controlled experiments *in vitro* using cadaveric human lungs and *in vivo* using murine flank tumors and confirmed that OTL38 had decreased auto-fluorescence and increased depth of penetration compared to EC17.(19, 34) We also demonstrated that OTL38 had high specificity for FRα-expressing tumor cells

lines *in vitro*, that OTL38 localized to murine lung cancer xenografts and spontaneous lung cancers in dogs *in vivo*, and that tumor margins correlated with fluorescence.(34, 35)

Clinical Applications

Identification of Small Nodules and Synchronous Disease

A major challenge in surgery for pulmonary malignancies is localization of small nodules and detection of synchronous or metachronous disease. This has become even more relevant with the increased use of video assisted thoracoscopic surgery (VATS), which does not allow tactile feedback. In the early VATS experience, Suzuki et al. found a 54% need for conversion from VATS to thoracotomy that increased to 63% for nodules ≤10 mm in size and > 5 mm from the pleural surface. Conversions were primarily due to inability to locate small nodules.(36) In a more contemporary series of non-small cell lung cancer patients who underwent open thoracotomy but had tumors amenable to resection by VATS, 8.4% had metastatic nodules in other lung lobes that would not have been discovered by VATS.(37)

Several other preoperative and intraoperative localization methods exist to improve intraoperative identification of small nodules.(38) Preoperative localization methods include placement of small metal objects (wires, microcoils, or fiduciaries) or dyes (methylene blue, lipiodol, or technetium-99) under bronchoscopy or computed tomography (CT) guidance.(39–51) Intraoperative localization methods include the use of ultrasound, CT, and fluoroscopy.(50, 52–55) Disadvantages of these techniques include complications such as pneumothorax with the preoperative localization techniques, exposure to radiation with CT or fluoroscopy, and the expertise needed for pulmonary ultrasound. Conversely, IFI is safe, does not involve radiation exposure, and is easy for the surgeon to perform and interpret. IFI has the added benefit of the ability to detect synchronous disease, which would not be possible without manual palpation with most of these other techniques.

TumorGlow® can detect Pulmonary Nodules—In our first clinical trial, we evaluated the ability of TumorGlow® to localize solitary pulmonary nodules.(56) In a study of 18 patients with a pulmonary nodule requiring resection by thoracotomy, TumorGlow® identified 14 out of 18 primary nodules *in situ*. The smallest nodule detected was 0.2 cm, and an additional 5 cancerous nodules were detected with TumorGlow® that were not evident on preoperative cross-sectional imaging, all of which were sub-centimeter in size. Three of these nodules were in different lobes than the primary lesion. Two of the nodules that did not fluoresce *in vivo* were fluorescent after they were bisected on the back table. The average depth of these nodules from the pleural surface was 1.7 cm, while the average depth of nodules that fluoresced *in vivo* was 0.4 cm. The two nodules seen preoperatively that were not identified by TumorGlow® were a metastatic melanoma and a pulmonary embolus. This trial demonstrated that TumorGlow® can detect small pulmonary nodules and find synchronous disease, and that one of the biggest limitations of IFI is depth of penetration.

A second proof of principal study in 5 patients demonstrated the other major limitation of TumorGlow®, which is suboptimal specificity due to dye accumulation in areas of inflammation.(18) In this study, 4 patients had relatively small tumors with no surrounding

inflammation, while one patient had a large tumor with distal obstructed lung. In each patient, the suspected margin was marked both by finger palpation and by NIR imaging. On pathology review, both NIR imaging and finger palpation accurately identified the margin for the small tumors without inflammation, but in the patient with a large tumor and inflammation, finger palpation underestimated the true extent of the tumor while NIR imaging identified a large section of atelectatic lung with no tumor cells.

These results with an ICG dose of 5 mg/kg and imaging 24 hours after infusion have recently been replicated by Mao et al.(57) In their study, NIR imaging with second window ICG identified 68 out of 76 nodules in 36 patients. All nodules not detected with imaging were at least 1.3 cm deep to the pleural surface. As was seen in our experience, they found that NIR imaging with second window ICG could detect sub-centimeter nodules and that additional lesions were found only with NIR imaging. Kim et al. reported the identification of pulmonary neoplasms with NIR imaging using an ICG dose of 1 mg/kg 24 hours prior to surgery in 11 patients.(58) Tumor fluorescence was seen in 8/9 patients with pulmonary neoplasms as well as in 2 patients who had no residual tumor but had post-obstructive pneumonitis following neoadjuvant chemoradiation. However, imaging in this study was only performed on the back table and not *in vivo*.

EC17 Improves Tumor Specificity but Sacrifices Depth of Penetration—Building on the promising results for pulmonary nodule detection with TumorGlow®, we subsequently used the folate-receptor targeted agent, EC17, to identify pulmonary adenocarcinomas in a clinical trial. In our initial study, we enrolled only patients with biopsy proven pulmonary adenocarcinoma. IFI with EC17 correctly identified 46 out of 50 lung adenocarcinomas; the four tumors that were not identified did not express FRα.(59) However, the fluorescence of EC17 within the visible spectrum further exacerbated the limitations related to depth of penetration. Due to limited depth of penetration, only 7 of the 50 tumors in this study were seen *in vivo*; the rest were fluorescent only after they were bisected. While the inability to see tumors *in vivo* was a major limitation to finding small nodules and synchronous disease, the high specificity observed suggested another application for targeted IFI, which is rapid pathologic diagnosis.

Therefore, we proceeded with a second study in which 30 patients with indeterminate pulmonary nodules underwent IFI with EC17 to determine the accuracy of EC17 in rapid intraoperative identification or “optical biopsy” of primary pulmonary adenocarcinomas.(60) In this study, IFI identified 19/30 nodules. Frozen section pathology results for the fluorescent nodules were 13 pulmonary adenocarcinomas, 4 cancers of unknown origin, 1 squamous cell carcinoma, and 1 benign lesion. Based on the frozen section results, 18/19 patients underwent a lobectomy. However, on final pathology, all 19 fluorescent nodules were pulmonary adenocarcinomas. Of most significance, the patient with a fluorescent tumor but a benign frozen section diagnosis received a wedge resection instead of a lobectomy and ultimately needed a second surgery for formal lobectomy. Frozen section pathology results for the 11 nodules that did not fluoresce were 5 benign nodules, 4 carcinomas of unknown origin, and 2 metastatic renal cell carcinomas. Final pathology demonstrated 3 non-caseating granulomas, 2 primary squamous cell carcinomas, 2 hamartomas, 2 metastatic renal cell carcinomas, 1 metastatic leiomyosarcoma, and 1

mucoepidermoid carcinoma. In summary, the sensitivity and specificity of optical biopsy with EC17 for pulmonary adenocarcinomas were both 100% (19/19 and 11/11, respectively). On average, optical biopsy took only 2.4 minutes compared to 26.5 minutes for standard frozen section, and it was more accurate in diagnosing pulmonary adenocarcinomas.

In these clinical studies with EC17, we noticed significant auto-fluorescence within the thoracic cavity.(61) The most auto-fluorescence was seen from the bronchus and pulmonary artery. While the auto-fluorescence could be improved by changing the image capture settings on the fluorescence imaging camera, it was not possible to eliminate auto-fluorescence from these structures. These data clearly demonstrated that a targeted NIR agent was needed.

OTL38 Improves Specificity Compared to TumorGlow® and Depth of Penetration Compared to EC17—In an attempt to improve depth of penetration and decrease auto-fluorescence in order to see more tumors *in vivo* while maintaining tumor specificity, we next evaluated OTL38 in a phase I clinical trial.(62) In our first 20 patients with biopsy proven pulmonary adenocarcinoma, we found 16/20 tumors were fluorescent *in vivo*, while all tumors were fluorescent *ex vivo*. The 4 tumors that were not fluorescent *in vivo* were deeper from the pleural surface. We also identified 4 sub-centimeter malignant nodules not seen on preoperative imaging.

Next, we evaluated the sensitivity and specificity of OTL38 for a variety of pulmonary nodule pathologies and determined the value that targeted IFI adds to preoperative ^{18}fluorodeoxyglucose positive emission tomography (FDG-PET). In a study of 50 patients, 92.0% (69/75) of total nodules and 95.6% (65/68) of malignant nodules were fluorescent.(63) IFI identified 94.9% (56/59) of malignant pulmonary nodules identified by FDG-PET but also found nodules that were not FDG-PET-avid in 18% (9/50) of patients and additional nodules not seen on preoperative FDG-PET in 12% (6/50) of patients. IFI was particularly helpful in identifying sub-centimeter malignant nodules, of which 100% (15/15) were fluorescent but only 26.7% (4/15) were FDG-PET-avid. Figure 1 shows an example of a sub-centimeter pulmonary adenocarcinoma *in situ* identified only with IFI. We hypothesized that fluorescent non-pulmonary adenocarcinoma nodules have low level FRα expression or accumulation of tumor associated macrophages, which express folate receptor-beta.(64) In a follow-up study of IFI with OTL38 for pulmonary squamous cell carcinomas, approximately 70% (9/13) of nodules accumulated OTL38.(65) All 9 nodules had FRα expression, albeit at low levels in 4 patients, suggesting low levels of FRα expression are sufficient for identification with OTL38. The efficacy of OTL38 is currently being further investigated in a 5-institution phase II clinical trial (NCT02872701). A summary of studies using IFI for pulmonary nodule detection after injection of systemic contrast agents is shown in Table 1.

Pulmonary Metastasectomy

Prolonged survival can be seen after pulmonary metastasectomy in appropriately selected patients with a limited number of metastases.(66) During pulmonary metastasectomy, 18–20% of patients have an ipsilateral malignant nodule discovered by manual lung palpation

that was not imaged preoperatively.(67, 68) In an effort to improve the detection of pulmonary metastases during VATS, we evaluated the ability of TumorGlow® to detect pulmonary metastases in a pilot study. In this study, 9/11 metastatic lung lesions in 8 patients were fluorescent on NIR imaging.(69) Histologies included melanoma, osteosarcoma, renal cell carcinoma, chondrosarcoma, leiomyosarcoma, and colorectal carcinoma, which demonstrated that ICG will accumulate in a wide variety of tumor pathologies. The two lesions that were not fluorescent were once again deeper in the lung parenchyma (1.6 and 1.8 cm from the pleural surface). We have since demonstrated that TumorGlow® can detect colorectal cancer lung metastases as small as 0.2 cm (under review).

Several patients in our pilot study of TumorGlow® for pulmonary metastasectomy had sarcoma pulmonary metastases. Based on the results of these cases and others with TumorGlow® for chest wall and mediastinal sarcomas,(17, 70) we are now routinely using TumorGlow® for resection of sarcoma pulmonary metastases (unpublished data). OTL38 is also a promising agent for targeted IFI of osteosarcoma pulmonary metastases. Osteosarcomas frequently have upregulated FRα,(71, 72) and we discovered that targeted IFI with OTL38 can identify osteosarcoma pulmonary metastases.(73)

Practical Recommendations Regarding IFI for Pulmonary Nodules

Based on our experience with IFI for indeterminate pulmonary nodules, we provide practical recommendations. First, a contrast agent should be selected based on preoperative data. While EC17 had high specificity for pulmonary adenocarcinomas, the limited depth of penetration was a major limitation demonstrating that an NIR agent is a necessity for effective real-time IFI. The decision between OTL38 and TumorGlow® is primarily histology dependent based on the most likely preoperative diagnosis. For a biopsy proven pulmonary adenocarcinoma or squamous cell carcinoma, we recommend using OTL38. For a biopsy proven pulmonary metastasis in a patient undergoing pulmonary metastasectomy, we recommend using TumorGlow®. Patients with indeterminate pulmonary nodules are more challenging. In patients with a significant smoking history and a high probability of lung cancer, we recommend OTL38. This is for two reasons: 1) most lung cancers have upregulated FRα, and 2) ICG accumulation in areas of inflammation creates a large amount of background fluorescence in patients with a significant smoking history. In patients with pulmonary metastasis high on the differential, particularly in patients without a smoking history, we recommend TumorGlow®, which will accumulate in a more diverse group of solid tumor histologies. Table 2 summarizes the advantages of each contrast agent. A representative IFI case for pulmonary adenocarcinoma with each imaging agent is shown in Figure 2.

The second recommendation relates to management of a fluorescent nodule. Our practice is to resect all fluorescent nodules if it does change the scope of an operation. We have found a sufficient number of additional malignant nodules with both OTL38 and TumorGlow®. Currently, we still use frozen section diagnosis as the standard of care in the case of indeterminate pulmonary nodules. Although IFI has been more accurate than frozen section in some cases, we have enough false positives (primarily granulomas) with both OTL38 and TumorGlow® that we would not perform a lobectomy based on a fluorescent nodule in a

wedge resection alone. Likewise, we would not terminate the operation for a non-fluorescent nodule in a wedge resection as folate receptor expression is not 100% even in pulmonary adenocarcinomas. This practice will likely change in the near future as multiple or multiplexed dyes are used to better discriminate histology.

Identification of Sentinel Lymph Nodes

Appropriate sampling of thoracic lymph nodes is critical to accurate lung and esophageal cancer staging. It can be challenging to perform an appropriate lymphadenectomy in non-small cell lung cancer due to a propensity for skip metastases to N2 nodal stations in the mediastinum and poor FDG-PET accuracy for lymph nodes smaller than 1 cm.(74–76) In esophageal cancer, locoregional lymph node metastases can be seen even after extensive lymphadenectomy.(77) Failure to give appropriate adjuvant therapy for lymph node metastases due to inaccurate or incomplete lymph node sampling could lead to recurrence. Therefore, there is significant interest in thoracic surgery to identify sentinel lymph nodes to ensure proper staging. Trials of lymph node staging modalities that do not use fluorescent dyes have had limited success.(78)

The feasibility of real-time sentinel lymph node mapping in lung cancer using IFI with ICG was first reported in 2011 by Yamashita et al.(79) They gave a peritumoral injection of 10 mg ICG followed by imaging immediately and 10 minutes after injection. They detected sentinel lymph nodes in 80.3% (49/61) of patients, and in 2 patients with positive lymph nodes, one had a false negative sentinel lymph node.(80) The most common reason for failing to identify a sentinel lymph node was ICG leakage from the injection site. In an IFI with ICG dose escalation trial by Gilmore et al., a peritumoral injection of 1000 μg ICG allowed detection of the sentinel lymph node in 80% (4/5) and 2500 μg allowed detection in 100% (4/4) of patients.(81)

Yuasa et al. were the first to use IFI with ICG for lymphadenectomy in esophageal cancer. (82) In this study, 0.5 ml of ICG was injected in two areas of the submucosa around the tumor. Fluorescent lymphatic channels and lymph nodes were then visualized. Sentinel lymph nodes were detected with ICG in 95% (19/20) of patients. In 4 patients with lymph node metastases, 1 had a false negative sentinel lymph node. In another study of 10 patients having submucosal peritumoral injection of ICG, 6/10 patients total but 5/5 patients given ICG:HSA had sentinel lymph nodes identified with IMI.(83) Overall lymph node status correlated with the status of the sentinel lymph node in all cases. In another recent study, 9 patients had a peritumoral injection of ICG for lymphadenectomy during esophagectomy. (84) There were 34 lymph node metastases in 3 patients. In all 3, there were lymph node metastases in the first nodal basin identified with ICG.

While these studies demonstrate the feasibility of sentinel lymph node identification after peritumoral injection of ICG, no group thus far has been successful in selectively identifying lymph nodes containing cancer cells. Our group has tried three iterations of intravenously injected dyes with no success. Issues include depth of penetration, loss of fluorescence in pigmented lymph nodes, passive drainage of the dye through all lymphatic channels draining the tumor, and non-specific binding of targeted dyes to other receptors that are upregulated in lymph nodes. A tracer or combination of tracers that could be injected systemically and

allow identification of both the tumor and the sentinel lymph node and/or lymph nodes harboring metastases would be ideal.

Assessment of Resection Margins

Anterior mediastinal masses represent a diverse group of rare neoplasms. For most solid anterior mediastinal masses, the mainstay of treatment is complete surgical resection.(85) For malignant thymoma, one of the most common mediastinal masses, postoperative radiation is recommended for patients following R1 resection or R0 resection with pathology stage II or greater.(86) Achieving complete surgical resection of mediastinal masses can be challenging due to proximity to surrounding critical structures including the heart, great vessels, and phrenic nerve. We have demonstrated that TumorGlow® can improve visualization of thymomas and thymic carcinosarcomas in pilot studies.(70, 87) More complete surgical resections of these neoplasms could potentially decrease the need for postoperative radiation and improve dissection of the tumor while sparing the phrenic nerve and other critical mediastinal structures (Figure 3). A larger clinical trial of TumorGlow® for anterior mediastinal masses is ongoing.

Tumor Debulking

Malignant pleural mesothelioma is a highly lethal disease with median survival of approximately 7 months for all comers and 20 months for patients receiving trimodality therapy with surgery, chemotherapy, and radiation.(88) The best chance for prolonged survival is with complete surgical debulking of all macroscopic disease.(89) Identification of small mesothelioma deposits is therefore critical during surgery. We have demonstrated that TumorGlow® can localize additional deposits of mesothelioma not evident with visual inspection and finger palpation during pleurectomy and decortication (Figure 4).(16, 90) In the first eight patients of a human pilot study, intravenous ICG 5 mg/kg was given 24 hours prior to surgery. Surgeons then attempted to perform complete surgical debulking using only visual inspection and hand palpation. NIR imaging of the wound bed was performed after surgeons felt they had a complete debulking. In all 8 patients, additional disease deposits were identified with NIR imaging. There was a mean of 1.8 additional disease deposits per patient that ranged in size from 0.3–2.2 cm. A larger clinical trial to determine the effect of the addition of TumorGlow® to mesothelioma debulking on survival is ongoing. Table 3 summarizes the benefits and short-comings of each IFI agent used to date in thoracic malignancies.

Summary

Intraoperative fluorescence imaging is a new tool for the surgeon with numerous applications in thoracic surgical oncology. Phase I clinical trials have demonstrated IFI is feasible for small pulmonary nodule localization, metastasectomy, sentinel lymph node identification, mediastinal mass margin assessment, and mesothelioma debulking.

A non-specific NIR contrast agent, ICG, can be used to identify small pulmonary nodules, sentinel lymph nodes, tumor margins, and residual disease in the wound bed. ICG accumulation within tumors is by the EPR effect, while sentinel lymph nodes are visualized

through passive drainage following peritumoral injection of ICG. The major limitation of tumor imaging with ICG is suboptimal specificity with accumulation in areas of inflammation, while sentinel lymph node identification can be impaired by ICG leakage from the injection site. A significant percentage of sentinel lymph nodes were false negatives in lung and esophageal cancer sentinel lymph node mapping studies. This may be a limitation of any method of sentinel lymph node identification in these malignancies rather than a limitation of the imaging itself. Identification of new tracers that can target both primary tumors and metastatic lymph nodes is an important area for further investigation.

A targeted NIR contrast agent, OTL38, can improve identification of small lung nodules compared to ICG by specifically targeting pulmonary adenocarcinomas and other folate-receptor expressing tumors. OTL38 is particularly helpful in identifying sub-centimeter primary, synchronous, or metachronous pulmonary nodules, which are not typically identified on preoperative FDG-PET. For primary lung cancers and pulmonary metastases, this can prevent thoracotomy for manual lung palpation. A significant number of patients have their disease upstaged with the addition of IFI with OTL38; in the absence of IFI, these patients would not receive appropriate adjuvant treatment due to failure to identify synchronous disease.

One of the major limitations of IFI is depth of penetration. Dyes that fluoresce in the visible spectrum only penetrate through a few millimeters of tissue, while NIR dyes have a 1–2 cm maximum depth of penetration.(91, 92) Depth of penetration could potentially be improved by development of new fluorescent probes and imaging systems that target the second window near-infrared (NIR2) range of 950–1400 nm. There is decreased tissue scatter and auto-fluorescence at these wavelengths, which has improved detection of small, deep tumors in animal models.(93, 94) Depth of penetration may also be improved through the use of multispectral optoacoustic imaging (MSOT).(95, 96) MSOT uses laser excitation to generate sound waves, which are less susceptible than light to scatter, that are detected by ultrasound. Endogenous (oxyhemoglobin, deoxyhemoglobin, melanin) and exogenous contrast agents have unique signals on MSOT, and the relative amount of each agent can be used to determine benign versus malignant tissue.(97)

In conclusion, a number of pilot and phase I clinical trials have clearly demonstrated that IFI for thoracic malignancies is feasible. OTL38 is currently in a 4-institution phase II clinical trial to further evaluate efficacy. More phase II and III trials are needed to determine IFI efficacy, impact on patient outcomes, and overall clinical value. Other future research will involve the development of drugs targeted to other receptors that are upregulated in thoracic malignancies. As more fluorescent dyes are developed, a patient ultimately could be injected with a cocktail of imaging agents that would provide a rapid intraoperative diagnosis, significantly decrease the total operative time, decrease the rate of conversion to open procedures, and allow for a more complete oncologic surgery. This technology is applicable to all solid tumors and will be increasingly utilized as new tumor specific fluorescent contrast agents are developed and the sensitivity and usability of commercially available imaging systems continues to improve.

Acknowledgments

Funding Sources

PSL is on the Board of Directors at On Target Laboratories, manufacturers of OTL38.

SS was supported by the NIH (R01 CA193556).

References

1. Aliperti LA, Predina JD, Vachani A, et al. Local and systemic recurrence is the Achilles heel of cancer surgery. Ann Surg Oncol. 2011; 18(3):603–7. [PubMed: 21161729]
2. Lohman RF, Ozturk CN, Ozturk C, et al. An Analysis of Current Techniques Used for Intraoperative Flap Evaluation. Ann Plast Surg. 2015; 75(6):679–85. [PubMed: 25003438]
3. Keller DS, Ishizawa T, Cohen R, et al. Indocyanine green fluorescence imaging in colorectal surgery: overview, applications, and future directions. Lancet Gastroenterol Hepatol. 2017; 2(10): 757–66. [PubMed: 28895551]
4. Ishizawa T, Fukushima N, Shibahara J, et al. Real-time identification of liver cancers by using indocyanine green fluorescent imaging. Cancer. 2009; 115(11):2491–504. [PubMed: 19326450]
5. van der Vorst JR, Schaafsma BE, Hutteman M, et al. Near-infrared fluorescence-guided resection of colorectal liver metastases. Cancer. 2013; 119(18):3411–8. [PubMed: 23794086]
6. Yokoyama N, Otani T, Hashidate H, et al. Real-time detection of hepatic micrometastases from pancreatic cancer by intraoperative fluorescence imaging: preliminary results of a prospective study. Cancer. 2012; 118(11):2813–9. [PubMed: 21990070]
7. Troyan SL, Kianzad V, Gibbs-Strauss SL, et al. The FLARE intraoperative near-infrared fluorescence imaging system: a first-in-human clinical trial in breast cancer sentinel lymph node mapping. Ann Surg Oncol. 2009; 16(10):2943–52. [PubMed: 19582506]
8. Gilmore DM, Khullar OV, Gioux S, et al. Effective low-dose escalation of indocyanine green for near-infrared fluorescent sentinel lymph node mapping in melanoma. Ann Surg Oncol. 2013; 20(7): 2357–63. [PubMed: 23440551]
9. Madajewski B, Judy BF, Mouchli A, et al. Intraoperative near-infrared imaging of surgical wounds after tumor resections can detect residual disease. Clin Cancer Res. 2012; 18(20):5741–51. [PubMed: 22932668]
10. Jiang JX, Keating JJ, Jesus EM, et al. Optimization of the enhanced permeability and retention effect for near-infrared imaging of solid tumors with indocyanine green. Am J Nucl Med Mol Imaging. 2015; 5(4):390–400. [PubMed: 26269776]
11. Matsumura Y, Maeda H. A new concept for macromolecular therapeutics in cancer chemotherapy: mechanism of tumoritropic accumulation of proteins and the antitumor agent smancs. Cancer Res. 1986; 46(12 Pt 1):6387–92. [PubMed: 2946403]
12. Maeda H, Matsumura Y. EPR effect based drug design and clinical outlook for enhanced cancer chemotherapy. Adv Drug Deliv Rev. 2011; 63(3):129–30. [PubMed: 20457195]
13. Heneweer C, Holland JP, Divilov V, et al. Magnitude of enhanced permeability and retention effect in tumors with different phenotypes: 89Zr-albumin as a model system. J Nucl Med. 2011; 52(4): 625–33. [PubMed: 21421727]
14. Kosaka N, Mitsunaga M, Longmire MR, et al. Near infrared fluorescence-guided real-time endoscopic detection of peritoneal ovarian cancer nodules using intravenously injected indocyanine green. Int J Cancer. 2011; 129(7):1671–7. [PubMed: 21469142]
15. Keating JJ, Nims S, Venegas O, et al. Intraoperative imaging identifies thymoma margins following neoadjuvant chemotherapy. Oncotarget. 2016; 7(3):3059–67. [PubMed: 26689990]
16. Kennedy GT, Newton A, Predina J, et al. Intraoperative near-infrared imaging of mesothelioma. Transl Lung Cancer Res. 2017; 6(3):279–84. [PubMed: 28713673]
17. Holt D, Parthasarathy AB, Okusanya O, et al. Intraoperative near-infrared fluorescence imaging and spectroscopy identifies residual tumor cells in wounds. J Biomed Opt. 2015; 20(7):76002. [PubMed: 26160347]

18. Holt D, Okusanya O, Judy R, et al. Intraoperative near-infrared imaging can distinguish cancer from normal tissue but not inflammation. PLoS One. 2014; 9(7):e103342. [PubMed: 25072388]
19. De Jesus E, Keating JJ, Kularatne SA, et al. Comparison of Folate Receptor Targeted Optical Contrast Agents for Intraoperative Molecular Imaging. Int J Mol Imaging. 2015; 2015:469047. [PubMed: 26491562]
20. O'Shannessy DJ, Yu G, Smale R, et al. Folate receptor alpha expression in lung cancer: diagnostic and prognostic significance. Oncotarget. 2012; 3(4):414–25. [PubMed: 22547449]
21. Elnakat H, Ratnam M. Distribution, functionality and gene regulation of folate receptor isoforms: implications in targeted therapy. Adv Drug Deliv Rev. 2004; 56(8):1067–84. [PubMed: 15094207]
22. Dosio F, Milla P, Cattel L. EC-145, a folate-targeted Vinca alkaloid conjugate for the potential treatment of folate receptor-expressing cancers. Curr Opin Investig Drugs. 2010; 11(12):1424–33.
23. Low PS, Kularatne SA. Folate-targeted therapeutic and imaging agents for cancer. Curr Opin Chem Biol. 2009; 13(3):256–62. [PubMed: 19419901]
24. Ebel W, Routhier EL, Foley B, et al. Preclinical evaluation of MORAb-003, a humanized monoclonal antibody antagonizing folate receptor-alpha. Cancer Immun. 2007; 7:6. [PubMed: 17346028]
25. Spannuth WA, Sood AK, Coleman RL. Farletuzumab in epithelial ovarian carcinoma. Expert Opin Biol Ther. 2010; 10(3):431–7. [PubMed: 20092424]
26. Konner JA, Bell-McGuinn KM, Sabbatini P, et al. Farletuzumab, a humanized monoclonal antibody against folate receptor alpha, in epithelial ovarian cancer: a phase I study. Clin Cancer Res. 2010; 16(21):5288–95. [PubMed: 20855460]
27. Chilvers AS, Thomas MH. Methods for the localization of incompetent ankle perforating veins. Br Med J. 1970; 2(5709):577. [PubMed: 5526614]
28. Feindel W, Yamamoto YL, Hodge CP. Red cerebral veins and the cerebral steal syndrome. Evidence from fluorescein angiography and microregional blood flow by radioisotopes during excision of an angioma. J Neurosurg. 1971; 35(2):167–79. [PubMed: 5570779]
29. Ross AJ 3rd, O'Neill JA Jr, Silverman DG, et al. A new technique for evaluating cutaneous vascularity in complicated conjoined twins. J Pediatr Surg. 1985; 20(6):743–6. [PubMed: 4087104]
30. Keating JJ, Okusanya OT, De Jesus E, et al. Intraoperative Molecular Imaging of Lung Adenocarcinoma Can Identify Residual Tumor Cells at the Surgical Margins. Mol Imaging Biol. 2016; 18(2):209–18. [PubMed: 26228697]
31. Hoogstins CE, Tummers QR, Gaarenstroom KN, et al. A Novel Tumor-Specific Agent for Intraoperative Near-Infrared Fluorescence Imaging: A Translational Study in Healthy Volunteers and Patients with Ovarian Cancer. Clin Cancer Res. 2016; 22(12):2929–38. [PubMed: 27306792]
32. Jacques SL. Optical properties of biological tissues: a review. Phys Med Biol. 2013; 58(11):R37–61. [PubMed: 23666068]
33. Gioux S, Choi HS, Frangioni JV. Image-guided surgery using invisible near-infrared light: fundamentals of clinical translation. Mol Imaging. 2010; 9(5):237–55. [PubMed: 20868625]
34. Predina JD, Newton AD, Connolly C, et al. Identification of a Folate Receptor-Targeted Near-Infrared Molecular Contrast Agent to Localize Pulmonary Adenocarcinomas. Mol Ther. 2017
35. Keating JJ, Runge JJ, Singhal S, et al. Intraoperative near-infrared fluorescence imaging targeting folate receptors identifies lung cancer in a large-animal model. Cancer. 2017; 123(6):1051–60. [PubMed: 28263385]
36. Suzuki K, Nagai K, Yoshida J, et al. Video-assisted thoracoscopic surgery for small indeterminate pulmonary nodules: indications for preoperative marking. Chest. 1999; 115(2):563–8. [PubMed: 10027460]
37. Cerfolio RJ, Bryant AS. Is palpation of the nonresected pulmonary lobe(s) required for patients with non-small cell lung cancer? A prospective study. J Thorac Cardiovasc Surg. 2008; 135(2): 261–8. [PubMed: 18242247]
38. Keating J, Singhal S. Novel Methods of Intraoperative Localization and Margin Assessment of Pulmonary Nodules. Semin Thorac Cardiovasc Surg. 2016; 28(1):127–36. [PubMed: 27568150]

39. Eichfeld U, Dietrich A, Ott R, et al. Video-assisted thoracoscopic surgery for pulmonary nodules after computed tomography-guided marking with a spiral wire. Ann Thorac Surg. 2005; 79(1): 313–6. discussion 6–7. [PubMed: 15620965]
40. Miyoshi K, Toyooka S, Gobara H, et al. Clinical outcomes of short hook wire and suture marking system in thoracoscopic resection for pulmonary nodules. Eur J Cardiothorac Surg. 2009; 36(2): 378–82. [PubMed: 19414272]
41. Dendo S, Kanazawa S, Ando A, et al. Preoperative localization of small pulmonary lesions with a short hook wire and suture system: experience with 168 procedures. Radiology. 2002; 225(2):511–8. [PubMed: 12409589]
42. Gonfiotti A, Davini F, Vaggelli L, et al. Thoracoscopic localization techniques for patients with solitary pulmonary nodule: hookwire versus radio-guided surgery. Eur J Cardiothorac Surg. 2007; 32(6):843–7. [PubMed: 17913505]
43. Ichinose J, Kohno T, Fujimori S, et al. Efficacy and complications of computed tomography-guided hook wire localization. Ann Thorac Surg. 2013; 96(4):1203–8. [PubMed: 23895891]
44. Powell TI, Jangra D, Clifton JC, et al. Peripheral lung nodules: fluoroscopically guided video-assisted thoracoscopic resection after computed tomography-guided localization using platinum microcoils. Ann Surg. 2004; 240(3):481–8. discussion 8–9. [PubMed: 15319719]
45. Mayo JR, Clifton JC, Powell TI, et al. Lung nodules: CT-guided placement of microcoils to direct video-assisted thoracoscopic surgical resection. Radiology. 2009; 250(2):576–85. [PubMed: 19188326]
46. Sancheti MS, Lee R, Ahmed SU, et al. Percutaneous fiducial localization for thoracoscopic wedge resection of small pulmonary nodules. Ann Thorac Surg. 2014; 97(6):1914–8. discussion 9. [PubMed: 24725836]
47. Lenglinger FX, Schwarz CD, Artmann W. Localization of pulmonary nodules before thoracoscopic surgery: value of percutaneous staining with methylene blue. AJR Am J Roentgenol. 1994; 163(2): 297–300. [PubMed: 7518642]
48. McConnell PI, Feola GP, Meyers RL. Methylene blue-stained autologous blood for needle localization and thoracoscopic resection of deep pulmonary nodules. J Pediatr Surg. 2002; 37(12): 1729–31. [PubMed: 12483642]
49. Watanabe K, Nomori H, Ohtsuka T, et al. Usefulness and complications of computed tomography-guided lipiodol marking for fluoroscopy-assisted thoracoscopic resection of small pulmonary nodules: experience with 174 nodules. J Thorac Cardiovasc Surg. 2006; 132(2):320–4. [PubMed: 16872957]
50. Nomori H, Horio H, Naruke T, et al. Fluoroscopy-assisted thoracoscopic resection of lung nodules marked with lipiodol. Ann Thorac Surg. 2002; 74(1):170–3. [PubMed: 12118752]
51. Chella A, Lucchi M, Ambrogi MC, et al. A pilot study of the role of TC-99 radionuclide in localization of pulmonary nodular lesions for thoracoscopic resection. Eur J Cardiothorac Surg. 2000; 18(1):17–21. [PubMed: 10869935]
52. Kondo R, Yoshida K, Hamanaka K, et al. Intraoperative ultrasonographic localization of pulmonary ground-glass opacities. J Thorac Cardiovasc Surg. 2009; 138(4):837–42. [PubMed: 19660350]
53. Piolanti M, Coppola F, Papa S, et al. Ultrasonographic localization of occult pulmonary nodules during video-assisted thoracic surgery. Eur Radiol. 2003; 13(10):2358–64. [PubMed: 12736756]
54. Santambrogio R, Montorsi M, Bianchi P, et al. Intraoperative ultrasound during thoracoscopic procedures for solitary pulmonary nodules. Ann Thorac Surg. 1999; 68(1):218–22. [PubMed: 10421144]
55. Gill RR, Zheng Y, Barlow JS, et al. Image-guided video assisted thoracoscopic surgery (iVATS) - phase I–II clinical trial. J Surg Oncol. 2015; 112(1):18–25. [PubMed: 26031893]
56. Okusanya OT, Holt D, Heitjan D, et al. Intraoperative near-infrared imaging can identify pulmonary nodules. Ann Thorac Surg. 2014; 98(4):1223–30. [PubMed: 25106680]
57. Mao Y, Chi C, Yang F, et al. The identification of sub-centimetre nodules by near-infrared fluorescence thoracoscopic systems in pulmonary resection surgeries. Eur J Cardiothorac Surg. 2017; 52(6):1190–6. [PubMed: 28950327]

58. Kim HK, Quan YH, Choi BH, et al. Intraoperative pulmonary neoplasm identification using near-infrared fluorescence imaging. Eur J Cardiothorac Surg. 2016; 49(5):1497–502. [PubMed: 26503731]
59. Okusanya OT, DeJesus EM, Jiang JX, et al. Intraoperative molecular imaging can identify lung adenocarcinomas during pulmonary resection. J Thorac Cardiovasc Surg. 2015; 150(1):28–35. e1. [PubMed: 26126457]
60. Kennedy GT, Okusanya OT, Keating JJ, et al. The Optical Biopsy: A Novel Technique for Rapid Intraoperative Diagnosis of Primary Pulmonary Adenocarcinomas. Ann Surg. 2015; 262(4):602–9. [PubMed: 26366539]
61. Predina JD, Okusanya O, A DN, et al. Standardization and Optimization of Intraoperative Molecular Imaging for Identifying Primary Pulmonary Adenocarcinomas. Mol Imaging Biol. 2018; 20(1):131–8. [PubMed: 28497233]
62. Predina JD, Newton AD, Keating J, et al. A Phase I Clinical Trial of Targeted Intraoperative Molecular Imaging for Pulmonary Adenocarcinomas. Ann Thorac Surg. 2018
63. Predina JD, Newton AD, Keating J, et al. Intraoperative Molecular Imaging Combined With Positron Emission Tomography Improves Surgical Management of Peripheral Malignant Pulmonary Nodules. Ann Surg. 2017; 266(3):479–88. [PubMed: 28746152]
64. Shen J, Putt KS, Visscher DW, et al. Assessment of folate receptor-beta expression in human neoplastic tissues. Oncotarget. 2015; 6(16):14700–9. [PubMed: 25909292]
65. Predina JD, Newton AD, Xia L, et al. An open label trial of folate receptor-targeted intraoperative molecular imaging to localize pulmonary squamous cell carcinomas. Oncotarget. 2018; 9(17): 13517–29. [PubMed: 29568374]
66. Pastorino U, Buyse M, Friedel G, et al. Long-term results of lung metastasectomy: prognostic analyses based on 5206 cases. J Thorac Cardiovasc Surg. 1997; 113(1):37–49. [PubMed: 9011700]
67. Cerfolio RJ, McCarty T, Bryant AS. Non-imaged pulmonary nodules discovered during thoracotomy for metastasectomy by lung palpation. Eur J Cardiothorac Surg. 2009; 35(5):786–91. discussion 91. [PubMed: 19237294]
68. Cerfolio RJ, Bryant AS, McCarty TP, et al. A prospective study to determine the incidence of non-imaged malignant pulmonary nodules in patients who undergo metastasectomy by thoracotomy with lung palpation. Ann Thorac Surg. 2011; 91(6):1696–700. discussion 700-1. [PubMed: 21619965]
69. Keating J, Newton A, Venegas O, et al. Near-Infrared Intraoperative Molecular Imaging Can Locate Metastases to the Lung. Ann Thorac Surg. 2017; 103(2):390–8. [PubMed: 27793401]
70. Predina JD, Newton AD, Desphande C, et al. Near-infrared intraoperative imaging during resection of an anterior mediastinal soft tissue sarcoma. Mol Clin Oncol. 2018; 8(1):86–8. [PubMed: 29387401]
71. Yang R, Kolb EA, Qin J, et al. The folate receptor alpha is frequently overexpressed in osteosarcoma samples and plays a role in the uptake of the physiologic substrate 5-methyltetrahydrofolate. Clin Cancer Res. 2007; 13(9):2557–67. [PubMed: 17473184]
72. Kansara M, Teng MW, Smyth MJ, et al. Translational biology of osteosarcoma. Nat Rev Cancer. 2014; 14(11):722–35. [PubMed: 25319867]
73. Predina JD, Newton A, Deshpande C, et al. Utilization of targeted near-infrared molecular imaging to improve pulmonary metastasectomy of osteosarcomas. J Biomed Opt. 2018; 23(1):1–4.
74. Yoshino I, Yokoyama H, Yano T, et al. Skip metastasis to the mediastinal lymph nodes in non-small cell lung cancer. Ann Thorac Surg. 1996; 62(4):1021–5. [PubMed: 8823083]
75. Takizawa T, Terashima M, Koike T, et al. Mediastinal lymph node metastasis in patients with clinical stage I peripheral non-small-cell lung cancer. J Thorac Cardiovasc Surg. 1997; 113(2): 248–52. [PubMed: 9040617]
76. Bille A, Pelosi E, Skanjeti A, et al. Preoperative intrathoracic lymph node staging in patients with non-small-cell lung cancer: accuracy of integrated positron emission tomography and computed tomography. Eur J Cardiothorac Surg. 2009; 36(3):440–5. [PubMed: 19464906]
77. Lerut T, Nafteux P, Moons J, et al. Three-field lymphadenectomy for carcinoma of the esophagus and gastroesophageal junction in 174 R0 resections: impact on staging, disease-free survival, and

outcome: a plea for adaptation of TNM classification in upper-half esophageal carcinoma. Ann Surg. 2004; 240(6):962–72. discussion 72-4. [PubMed: 15570202]

78. Tiffet O, Nicholson AG, Khaddage A, et al. Feasibility of the detection of the sentinel lymph node in peripheral non-small cell lung cancer with radio isotopic and blue dye techniques. Chest. 2005; 127(2):443–8. [PubMed: 15705980]
79. Yamashita S, Tokuishi K, Anami K, et al. Video-assisted thoracoscopic indocyanine green fluorescence imaging system shows sentinel lymph nodes in non-small-cell lung cancer. J Thorac Cardiovasc Surg. 2011; 141(1):141–4. [PubMed: 20392454]
80. Yamashita S, Tokuishi K, Miyawaki M, et al. Sentinel node navigation surgery by thoracoscopic fluorescence imaging system and molecular examination in non-small cell lung cancer. Ann Surg Oncol. 2012; 19(3):728–33. [PubMed: 22101727]
81. Gilmore DM, Khullar OV, Jaklitsch MT, et al. Identification of metastatic nodal disease in a phase 1 dose-escalation trial of intraoperative sentinel lymph node mapping in non-small cell lung cancer using near-infrared imaging. J Thorac Cardiovasc Surg. 2013; 146(3):562–70. discussion 9–70. [PubMed: 23790404]
82. Yuasa Y, Seike J, Yoshida T, et al. Sentinel lymph node biopsy using intraoperative indocyanine green fluorescence imaging navigated with preoperative CT lymphography for superficial esophageal cancer. Ann Surg Oncol. 2012; 19(2):486–93. [PubMed: 21792510]
83. Hachey KJ, Gilmore DM, Armstrong KW, et al. Safety and feasibility of near-infrared image-guided lymphatic mapping of regional lymph nodes in esophageal cancer. J Thorac Cardiovasc Surg. 2016; 152(2):546–54. [PubMed: 27179838]
84. Schlottmann F, Barbetta A, Mungo B, et al. Identification of the Lymphatic Drainage Pattern of Esophageal Cancer with Near-Infrared Fluorescent Imaging. J Laparoendosc Adv Surg Tech A. 2017; 27(3):268–71. [PubMed: 27992300]
85. Kondo K, Monden Y. Therapy for thymic epithelial tumors: a clinical study of 1,320 patients from Japan. Ann Thorac Surg. 2003; 76(3):878–84. discussion 84–5. [PubMed: 12963221]
86. National Comprehensive Cancer Network. NCCN Clinical Practice Guidelines in Oncology: Thymomas and Thymic Carcinomas NCCN Evidence Blocks Version 1. 2018
87. Keating J, Judy R, Newton A, et al. Near-infrared operating lamp for intraoperative molecular imaging of a mediastinal tumor. BMC Med Imaging. 2016; 16:15. [PubMed: 26883511]
88. Saddoughi SA, Abdelsattar ZM, Blackmon SH. National Trends in the Epidemiology of Malignant Pleural Mesothelioma: A National Cancer Data Base Study. Ann Thorac Surg. 2018; 105(2):432–7. [PubMed: 29223422]
89. Marulli G, Breda C, Fontana P, et al. Pleurectomy-decortication in malignant pleural mesothelioma: are different surgical techniques associated with different outcomes? Results from a multicentre study. Eur J Cardiothorac Surg. 2017; 52(1):63–9. [PubMed: 28419212]
90. Predina JD, Newton A, Kennedy G, et al. Near-Infrared Intraoperative Imaging Can Successfully Identify Malignant Pleural Mesothelioma After Neoadjuvant Chemotherapy. Mol Imaging. 2017; 16 1536012117723785.
91. Vahrmeijer AL, Hutteman M, van der Vorst JR, et al. Image-guided cancer surgery using near-infrared fluorescence. Nat Rev Clin Oncol. 2013; 10(9):507–18. [PubMed: 23881033]
92. de Boer E, Harlaar NJ, Taruttis A, et al. Optical innovations in surgery. Br J Surg. 2015; 102(2):e56–72. [PubMed: 25627136]
93. Welsher K, Sherlock SP, Dai H. Deep-tissue anatomical imaging of mice using carbon nanotube fluorophores in the second near-infrared window. Proc Natl Acad Sci U S A. 2011; 108(22):8943–8. [PubMed: 21576494]
94. Ghosh D, Bagley AF, Na YJ, et al. Deep, noninvasive imaging and surgical guidance of submillimeter tumors using targeted M13-stabilized single-walled carbon nanotubes. Proc Natl Acad Sci U S A. 2014; 111(38):13948–53. [PubMed: 25214538]
95. Tzoumas S, Nunes A, Olefir I, et al. Eigenspectra optoacoustic tomography achieves quantitative blood oxygenation imaging deep in tissues. Nat Commun. 2016; 7:12121. [PubMed: 27358000]
96. Brochu FM, Brunker J, Joseph J, et al. Towards Quantitative Evaluation of Tissue Absorption Coefficients Using Light Fluence Correction in Optoacoustic Tomography. IEEE Trans Med Imaging. 2017; 36(1):322–31. [PubMed: 27623576]

97. McNally LR, Mezera M, Morgan DE, et al. Current and Emerging Clinical Applications of Multispectral Optoacoustic Tomography (MSOT) in Oncology. Clin Cancer Res. 2016; 22(14): 3432–9. [PubMed: 27208064]

Synopsis

In this review, we summarize the preclinical and clinical data on intraoperative fluorescence imaging in thoracic surgery.

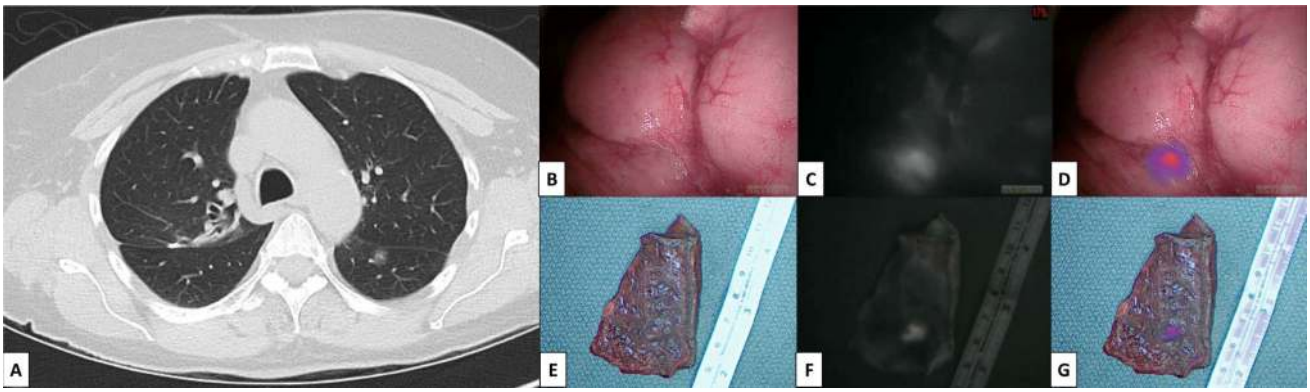

Figure 1.

A) Preoperative CT scan demonstrating left lower lobe ground glass opacity. *In vivo* images of left lower lobe lung nodule 4 hours after 0.025 mg/kg infusion of OTL38 on B) white light, C) near-infrared light, and D) near-infrared overlay imaging. Back table images of lung wedge resection specimen on E) white light, F) near-infrared light, and G) near-infrared overlay imaging. Final pathology demonstrated a 0.6 cm adenocarcinoma *in situ*.

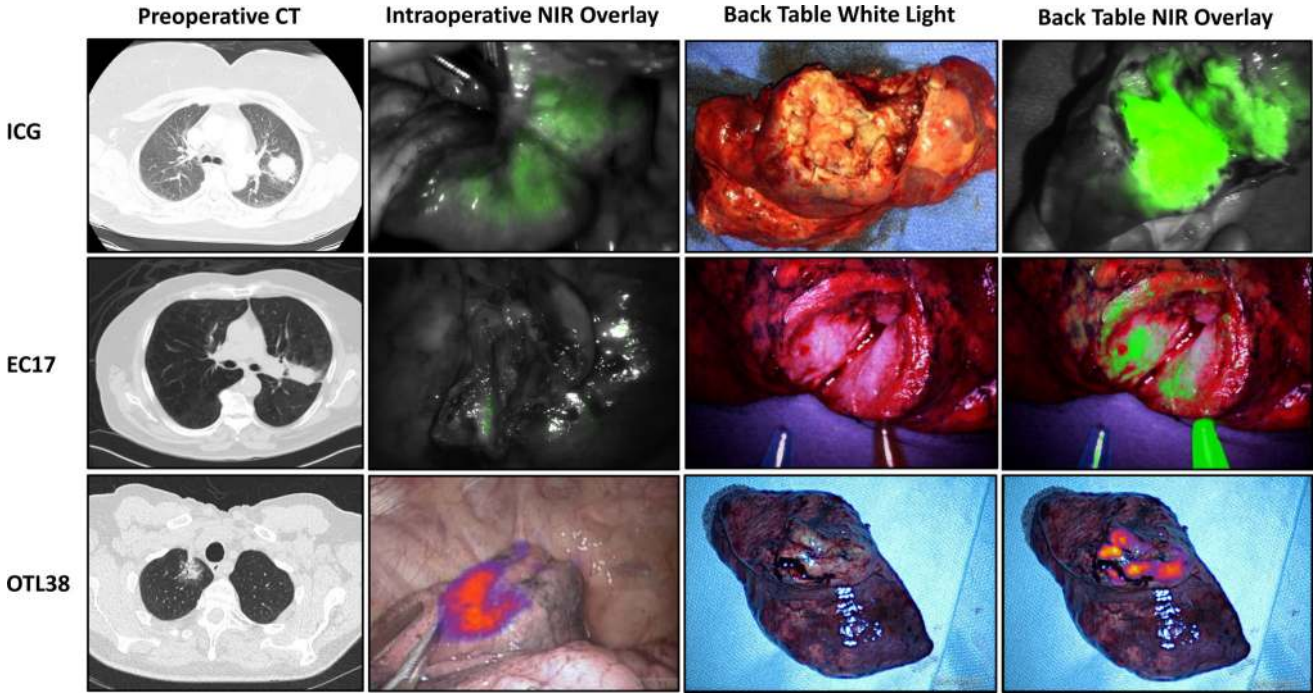

Figure 2.
Comparison of intraoperative and back table fluorescence imaging for pulmonary adenocarcinoma with ICG, EC17, and OTL38.

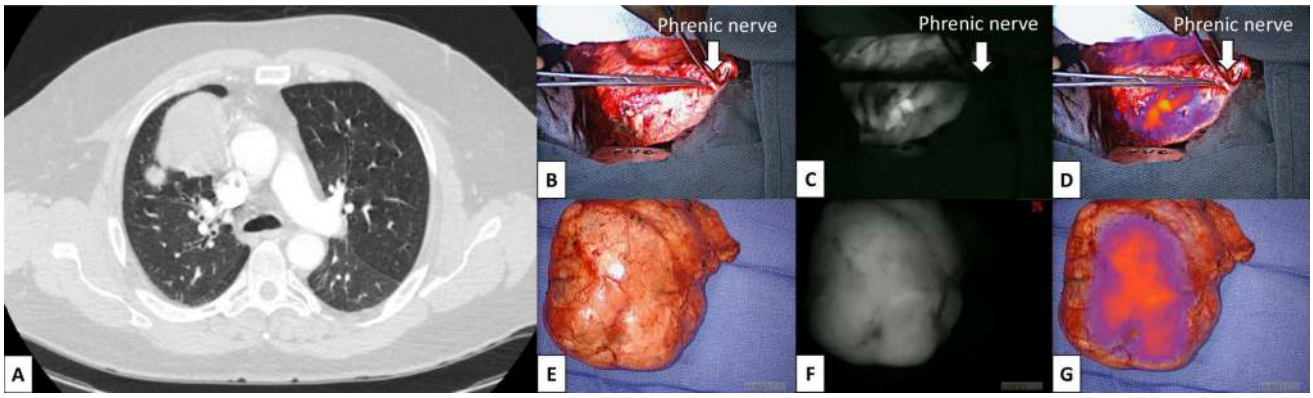

Figure 3.

A) Preoperative CT scan demonstrating an anterior mediastinal mass. *In vivo* images of thymoma resection 24 hours after 5 mg/kg ICG infusion on B) white light, C) near-infrared light, and D) near-infrared overlay imaging. Back table images of resected thymoma specimen with E) white light, F) near-infrared light, and G) overlay imaging. Final pathology demonstrated an encapsulated thymoma WHO type AB.

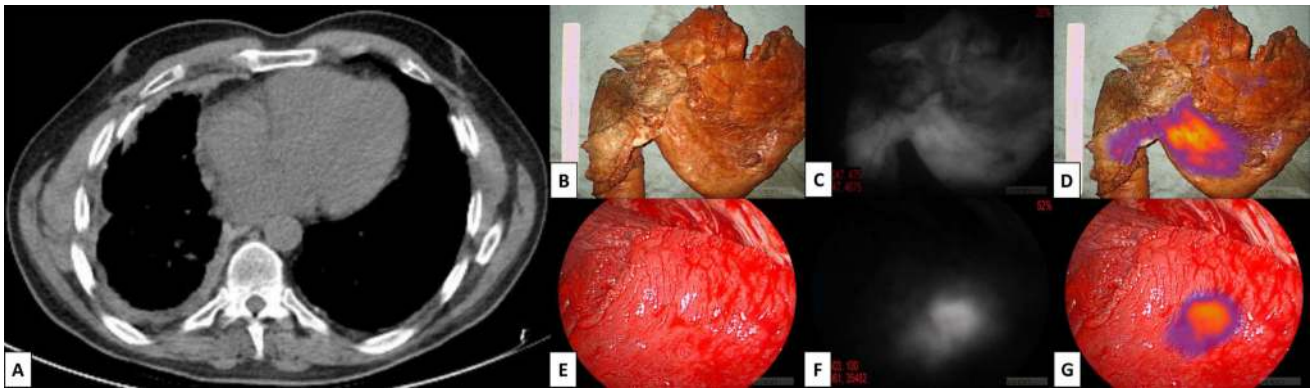

Figure 4.

A) Preoperative CT scan demonstrating right sided pleural thickening. Back table images of resected pleural peel during pleurectomy and decortication 24 hours after 5 mg/kg ICG infusion on B) white light, C) near-infrared light, and D) overlay imaging. *In vivo* images of residual visceral pleural mesothelioma deposit during pleurectomy and decortication on E) white light, F) near-infrared light, and G) overlay imaging.

J Surg Oncol. Author manuscript; available in PMC 2019 August 11.

Table 1

Summary of clinical trials of intraoperative fluorescence imaging for pulmonary nodules following systemic injection of a fluorescent contrast agent.

Study Drug	Study	Year	Dose (mg/kg)	Time from Injection to Imaging (hours)	No. of Patients	Sensitivity for Malignancy	Specificity for Malignancy	For Fluorescent Nodules, % Fluorescent *in vivo*	Smallest Nodule Detected (cm)	Maximum Depth of Penetration (cm)	Major Findings of Study
ICG	Okusanya et al.(56)	2014	5	24	18	95.5% (21/22)	100% (1/1)	66.7% (14/21)	0.2	1.3	ICG can locate pulmonary nodules, including nodules not identified on preoperative imaging.
	Kim et al.(58)	2016	1	24	11	88.9% (8/9)	0% (0/2)	NR	0.3	1.4	ICG can locate pulmonary nodules in resected lung specimens at a 1 mg/kg dose. Two false positives seen in patients with no residual tumor after neoadjuvant treatment.
	Keating et al.(69)	2017	5	24	8	81.8% (9/11)	N/A	100% (9/9)	NR	NR	ICG can locate pulmonary metastases, including nodules not identified on preoperative imaging.
	Mao et al.(57)	2017	5	24	36	88.7% (63/71)	0% (0/5)	100% (68/68)	0.1	1.3	ICG can locate both primary lung cancers and pulmonary metastases during VATS.
EC17	Okusanya et al.(59)	2015	0.1	4	50	92.3% (48/52)	N/A	15.4% (8/52)	0.3	0	EC17 had 92% sensitivity for pulmonary adenocarcinomas. Only 14% of nodules were identified with IFI *in vivo*.
	Kennedy et al.(60)	2015	0.1	4	30	100%* (19/19)	100%* (11/11)	NR	0.7	0	EC17 had 100% specificity for pulmonary adenocarcinomas. Optical biopsy was more accurate than frozen section for pulmonary adenocarcinomas identification.
OTL38	Predina et al.(62)	2018	0.025	3–6	20	100% (24/24)	N/A	83.3% (20/24)	0.1	2.0	OTL38 can locate pulmonary adenocarcinomas and identifies more nodules *in vivo* than EC17.
	Predina et al.(63)	2017	0.025	3–6	50	95.6% (65/68)	42.9% (3/7)	NR	0.2	2.0	IFI with OTL38 was 100% sensitive for sub-centimeter malignant pulmonary nodules while FDG-PET was only 26.6% sensitive.
	Predina et al. (65)	2018	0.025	3–6	12	69.2% (9/13)	N/A	100% (9/9)	1.1	1.2	OTL38 identified ~70% of squamous cell carcinomas. Only low levels of FRα expression were needed for fluorescence.

*Sensitivity and specificity reported for pulmonary adenocarcinomas rather than all malignant nodules.

Abbreviations: No., number; ICG, indocyanine green; IFI, intraoperative fluorescence imaging; NR, not reported; VATS, video assisted thoracoscopic surgery; FDG-PET, ^{18}fluorodeoxyglucose positive emission tomography

Table 2

Advantages of TumorGlow®, EC17, and OTL38 for IFI of Pulmonary Nodules

	Depth of Penetration	Lack of Autofluorescence	Sensitivity	Specificity
TumorGlow®	++	+++	+++	+
EC17	+	+	+	+++
OTL38	+++	+++	++	++

Table 3

Summary of contrast agent, tumor type, advantages over standard of care, and short-comings of intraoperative fluorescence imaging in thoracic surgery.

Agent	Tumor Type	Current Standard of Care	Benefits of IFI	Short-comings
ICG	**Pulmonary nodules**	Manual palpation if not identified by VATS	• Detects unidentified nodules • Avoids thoracotomies	• Limited depth of penetration • Poor specificity
	NSCLC sentinel lymph nodes	Complete lymphadenectomy or lymph node sampling	• Accurate lymph node sampling	• Failure to identify sentinel lymph nodes due to ICG leakage • False negative sentinel lymph nodes
	Esophageal cancer sentinel lymph nodes	Limited lymphadenectomy (THE) or extended lymphadenectomy(TTE)	• Accurate lymph node sampling	• False negative sentinel lymph nodes
	Mediastinal masses	Visualization and palpation	• Visualization for minimally invasive procedures • Differentiation of tumor from critical structures	• Background fluorescence from the heart and great vessels
	Mesothelioma	Visualization and palpation	• Identifies additional disease deposits	• Poor specificity
EC17	**Pulmonary adenocarcinoma**	Frozen section pathology	• Improves accuracy over frozen section diagnosis • Decreases operating room time	• Poor depth of penetration • Only useful for pulmonary adenocarcinoma
OTL38	**Pulmonary adenocarcinoma**	Manual palpation if not identified by VATS	• Detects otherwise unidentified nodules • Avoids thoracotomies	• Limited depth of penetration
	Pulmonary squamous cell carcinoma	Manual palpation if not identified by VATS	• Avoids thoracotomies	• Limited depth of penetration • Only moderate FRα expression
	Pulmonary nodules	Manual palpation if not identified by VATS	• Detects otherwise unidentified nodules • Avoids thoracotomies	• Limited depth of penetration • Limited to nodules with folate receptor expression

Abbreviations: IFI intraoperative fluorescence imaging, ICG indocyanine green, VATS video assisted thoracoscopic surgery, THE transhiatal esophagectomy, TTE transthoracic esophagectomy, FRα folate receptor-alpha